Relationship Between 1 H Chemical Shifts of Deuterated Pyridinium Ions and Brønsted Acid Strength of Solid Acids

ARTICLE *in* THE JOURNAL OF PHYSICAL CHEMISTRY B · APRIL 2007

Impact Factor: 3.3 · DOI: 10.1021/jp067340c · Source: PubMed

ARTICLES

Relationship Between ^{1}H Chemical Shifts of Deuterated Pyridinium Ions and Brønsted Acid Strength of Solid Acids

Anmin Zheng, Hailu Zhang, Lei Chen, Yong Yue, Chaohui Ye, and Feng Deng*

State Key Laboratory of Magnetic Resonance and Atomic and Molecular Physics, Wuhan Institute of Physics and Mathematics, The Chinese Academy of Sciences, Wuhan 430071, People's Republic of China

Received: November 7, 2006; In Final Form: January 9, 2007

Deuterated pyridine (pyridine-d_5) is one of the NMR probe molecules widely used for determination of acid strength of solid catalysts. However, the correlation between the ^{1}H chemical shift of adsorbed pyridine-d_5 and the Brønsted acid strength of solid acids has rarely been investigated. Here, an 8T zeolite model with different Si−H bond lengths is used to represent the Brønsted acid sites with different strengths (from weak, strong, to superacid) and to predict the pyridine adsorption structure as well as the ^{1}H chemical shift. The theoretical calculation suggests that a smaller ^{1}H chemical shift of the pyridinium ions on the solid acids indicates a stronger acid strength. On the basis of the results of theoretical calculations, a linear correlation between the pyridine-d_5 ^{1}H chemical shift and the proton affinity (PA) of the Brønsted acid site has been derived. In combination with the available ^{1}H MAS NMR experimental data, we conclude that pyridine-d_5 can be used as a scale to characterize the solid acid strength.

Introduction

Solid acid catalysts (including zeolites, complex oxide, heteropoly acid, etc.) have been widely used in chemical and petrochemical processes, such as the transformation of methanol into hydrocarbons, isomerization of aromatic compounds, and cracking of *n*-alkanes.[1] Several spectroscopic methods such as IR, temperature-programmed desorption (TPD), microcalorimetry, and solid-state NMR are employed to characterize the acidity of solid acid catalysts.[2−6] Among them, solid-state NMR is a powerful tool to characterize the nature of different acid sites on solid acid catalysts. ^{1}H MAS NMR can provide structural information about various hydroxyl groups including the bridging OH groups (Brønsted acid site). Adsorption of probe molecules on the acidic catalysts is one of the methods widely used to characterize the solid acidity as well as the interactions between the base probe molecules and the acid sites.[3−6] Deuterated pyridine (pyridine-d_5) is usually used for determination of the acid property of surface OH groups.[7−10] The formation of a hydrogen bond between pyridine and a nonacidic hydroxyl group (such as Si−OH) shifts the ^{1}H MAS NMR signal position from 2 to about 10 ppm. In the case of acidic OH groups (Brønsted acid sites), the adsorption of pyridine results in ^{1}H NMR signals in the range of 12−20 ppm. The large downfield shift of the ^{1}H NMR signal results from a proton transfer from the acidic OH group to the probe molecule, forming a pyridinium ion.[7−11]

Although the ^{1}H MAS NMR of adsorbed pyridine-d_5 can be used to characterize the presence of Brønsted acid sites,[7−11] the relationship between the ^{1}H chemical shift and the Brønsted acid strength of solid acids is rarely investigated. Density functional theory (DFT) quantum chemical calculations offer a new opportunity to reveal the correlation. In this contribution, using a generic zeolite as an example, which is one kind of important solid acid used in the petrochemical industry, we have systematically investigated the pyridine absorption structures and calculated the ^{1}H chemical shifts of pyridine adsorbed on solid acids with different acid strengths with DFT calculations. A correlation between the ^{1}H chemical shift of adsorbed pyridinium ions and the proton affinity of solid acids is derived as well.

Computational Methods

It has been demonstrated by Kramer et al. and Zheng et al.[12−13] that the acid strength of zeolite catalysts can be simulated by modifying the peripheral Si−H bonds of the cluster model. In order to represent a series of solid acids with different strengths, 8T models of zeolite ZSM-5 with different terminal Si−H bond lengths were used. Zeolite ZSM-5 has two types of pores, both formed by 10-membered rings. The first type is a straight and elliptical channel, with a free cross-section of 5.5 × 5.1 Å. The second type is a sinusoidal channel with a cross-section of 5.6 × 5.4 Å. This unique three-dimensional pore structure allows a molecule to move freely into the catalyst.[14]

In our calculations, zeolite H−ZSM-5 was modeled by an 8T ($(H_3SiO)_3$−Si−OH−Al−$(SiOH_3)_3$) cluster model, the Al12−O24(H)−Si12 site was used to represent the Brønsted acid site of zeolite H−ZSM-5 (See Figure 1). This site was chosen because it is one of the most likely sites for Al substitution, and also it is located in the intersection of the straight channel and the sinusoidal channel of zeolite ZSM-5, a position readily accessible by adsorbents.[15−16] We used a partial optimization

* To whom correspondence should be addressed. Fax: 86-27-87199291. E-mail: dengf@wipm.ac.cn.

10.1021/jp067340c CCC: $37.00
Published on Web 03/07/2007

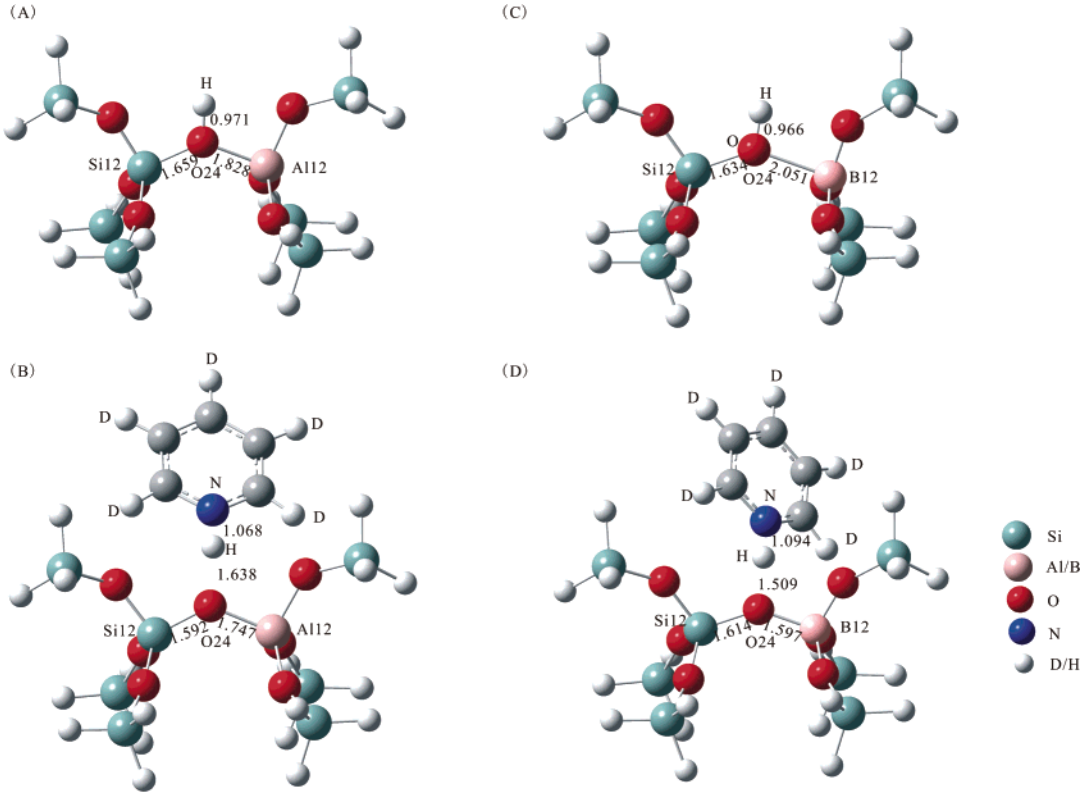

Figure 1. B3LYP/DZVP2-optimized zeolite structures and equilibrium configurations of pyridine adsorbed on the 8T models for Al−ZSM-5 (A and B) and B−ZSM-5 (C and D) zeolite. The interatomic distances (Å) are indicated.

with the O_3−Si−OH−Al−O_3 cluster relaxed while the angles of the H3 groups on the peripheral Si atoms were fixed to be aligned with the axes needed to connect Si to neighbor atoms in the real zeolite on the basis of crystallographic locations,[17] which can avoid losing the unique structure of zeolite ZSM-5 due to full optimization of the cluster. No atom in the pyridine molecule was constrained through all the configuration optimizations of adsorption complexes. The structure parameters of ZSM-5 used in the calculations were extracted from the crystal structural data of the ZSM-5 zeolite.[18] All of the terminal hydrogen atoms in the clusters are located at a Si−H distance of r Å from the corresponding silicon, orienting along the bond direction to the next oxygen atom in calculations. In order to investigate the correlation between the ^{1}H chemical shift of adsorbed pyridine-d_5 and the Brønsted acid strength of solid acids, we set r to 1.30, 1.40, 1.50, 1.60, 1.75, 2.00, 2.25, and 2.50 Å to represent eight solid acids with different strengths (from weak, strong to superacid). As demonstrated by our previous calculations, a Si−H bond length of 1.47 Å could represent the acid strengths of zeolites.[17b] In order to compare with experimental results, the calculation is also included for the Si−H bond length being 1.47 Å.

It is well-known that besides Al, many other elements such as B, Ga, and Fe can also replace Si in the zeolite framework, and the element substitution can modify the acid strength of zeolites.[19] We also studied the adsorption of pyridine on the acid sites of B−ZSM-5.

The geometrical parameters and Mulliken charge distributions of the zeolite and pyridine adsorption complexes were optimized at the DFT level using the Becke's three-parameter hybrid method with the Lee−Yang−Parr correlation functional (B3LYP) and the double ξ plus polarization basis set (DZVP2).[20] The single-point energies were calculated at the B3LYP/DZVP2 level with Basis Set Superposition Error (BSSE) correction on the optimized structures. ^{1}H isotropic chemical shifts of the adsorption complexes were calculated at the same theoretical level by the gauge-independent atomic orbital (GIAO) method. The DZVP2 basis set has been demonstrated to successfully predict the structure and NMR parameters of probe molecules adsorbed on zeolites.[17] The calculated ^{1}H chemical shift (17.7 ppm) at the B3LYP/DZVP2 level of pyridine-d_5 adsorbed on H−ZSM-5 (relative to the absolute shielding of liquid TMS at room temperature) was overestimated by +2.2 ppm compared with the experimental value (15.5 ppm).[10a] Therefore, the experimental chemical shift of pyridine-d_5 adsorbed on H−ZSM-5 was adopted as an internal standard for the conversion from the calculated isotopic absolute shielding constant to the final calculated chemical shift. In order to compare the effect of both computational methods and basis sets on the chemical shifts, we also used B3LYP/6-311g(d) and MP2/6-311g(d) methods to predict the ^{1}H isotropic chemical shifts. All calculations were performed using Gaussian03 program package.[21]

Results and Discussion

Proton affinity (PA) is a criterion to evaluate the intrinsic acidity strength of zeolites and other solid acids. The PA value can be obtained by comparing the energy difference between protonated and deprotonated zeolite models. The smaller the PA value, the more easily the Brønsted acidic proton can be deprotonated, and thus the much stronger the acid strength would be.[22]

It has been shown by Kramer et al. that the modulation of Brønsted acid strength can be done by modifying the peripheral Si−H bonds of the cluster model used in the DFT theoretical simulation.[12] This method has been widely used in the zeolite theoretical calculations.[12−13] As shown in Table 1, the acidic bridging O−H bond length increases slightly from 0.9704 to 0.9735 Å with the Si−H bond length increasing from 1.30 to 2.50 Å. Accordingly, the PA value decreases from 310.8 to 254

TABLE 1: Proton Affinity (PA) and O−H Bond Length (r_{O-H}) of the Bare Zeolites and the N−H Bond Length (r_{N-H}), Charge Distribution, and BSSE Corrected Adsorption Energies of Pyridine Adsorption Complexes Predicted at the B3LYP/DZVP2 Level on an 8T Cluster with the Si−H Bond Length Increasing from 1.30 to 2.50 Å

	bare zeolites		pyridine adsorption complexes			
$r_{(Si-H)}$	$r_{(O-H)}$	PA	r_{N-H}	$Q_{(H+)}$	$Q_{(pyridine-H+)}$	E_{ads}
1.30	0.9704	310.8	1.075	0.395	0.8959	22.9
1.40	0.9706	305.2	1.070	0.393	0.9030	24.9
1.47	0.9707	301.6	1.068	0.391	0.9052	26.1
1.50	0.9708	300.4	1.0666	0.389	0.9086	26.9
1.60	0.9711	294.9	1.063	0.384	0.9113	29.0
1.75	0.9716	286.5	1.057	0.378	0.9091	32.2
2.00	0.9724	273.8	1.048	0.364	0.9153	38.7
2.25	0.9730	263.0	1.041	0.3512	0.9142	43.6
2.50	0.9735	254.2	1.036	0.3405	0.9163	48.1

[a] Bond length in Å, adsorption energy in kcal/mol, and charge in |e|.

kcal/mol, which can cover the PA range of weak, strong, and superacids. All the variations (bond length and PA of the acidic O−H) indicate that the acid strength gradually increases with the increase of the Si−H bond length. When the Si−H bond length varies in the range of 1.47−1.50 Å, which is the bond length usually used to represent the zeolite structure in the theoretical calculations,[17,22−24] we find that the corresponding PA value falls in the range of 301.6−300.4 kcal/mol, which is in good agreement with the experimental value (291−300 kcal/mol) for zeolite ZSM-5.[25]

Because the pyridine molecule is a strong base probe, its adsorption on a Brønsted acid site will result in the formation of a pyridinium ion. For example, when the Si−H bond length is set to 1.47 Å, the most obvious change after the adsorption of pyridine is that the zeolite−OH bond length has been elongated from 0.971 Å in the bare zeolite to 1.638 Å in the adsorption complexes, whereas the N−H bond length has decreased to 1.068 Å (see Figure 1, parts A and B), indicative of the occurrence of proton transfer from the zeolite to pyridine, forming a pyridinium ion. As indicated in Table 1, with the Si−H bond length increasing from 1.30 to 2.50 Å, r_{N-H} gradually decreases from 1.075 to 1.036 Å with the latter being close to the N−H bond length of pyridine−H^+ ions in liquid superacid, which has a N−H bond length of 1.02 Å predicted at B3LYP/DZVP2 level.

Table 1 also lists the adsorption energy of pyridine on the zeolite. The adsorption energy ΔE_{ads} of pyridine on the zeolites was calculated as the energy difference between the absorbed complex system and the sum of the separated fragments:

$$\Delta E_{ads} = (E_{ZOH} + E_{pyridine}) - E_{pyridine-ZOH}$$

where $E_{pyridine-ZOH}$ represents the single-point energy of the optimized pyridine−ZOH complex, and E_{ZOH} and $E_{pyridine}$ are the single-point energies of the optimized bare zeolite and pyridine, respectively.

With the increase of acid strength, the adsorption energy increases from the 22.9 to 48.1 kcal/mol. It is noteworthy that with the increase of acid strength, the Mulliken charge distribution on the pyridine−H^+ fragment slightly increases, whereas the charge on the H^+ ion gradually decreases. As shown in Table 1, when the Si−H bond is equal to 1.3 Å, the Mulliken charge on the H^+ ion is 0.395 |e|, while when the Si−H bond is elongated to 2.50 Å, the charge decreases to 0.341 |e|. When pyridine is protonated by liquid superacid to form a fully protonated pyridine−H^+ ion, our calculation suggests that the charge on the H^+ ion is much less, only 0.286 |e|. This indicates that with the increase of acid strength, more and more positive charge is dispersed by the big conjugate ring of the pyridine molecule. Obviously, for the fully protonated pyridine−H^+ ion, the pyridine ring disperses more than 70% positive charge, while the H atom only holds less than 30% positive charge. Just because of the very pronounced electron-donor effect from the pyridine ring, the closer the distance is between the acidic proton and the N atom of pyridine, the more evident the electron-donor effect is, and thus the smaller the Mulliken charge is on the H^+ ion.

TABLE 2: ^{1}H Chemical Shift of Pyridine Adsorption Complexes Predicted at Different Levels on an 8T Cluster with the Si−H Bond Length Increasing from 1.30 to 2.50 Å

	^{1}H chemical shift (ppm)		
$r_{(Si-H)}$ (Å)	B3LYP/6-311g(d)	B3LYP/DZVP2	MP2/6-311g(d)[a]
1.30	16.0	16.2	16.1
1.40	15.7	15.8	15.8
1.47	15.5	15.5	15.5
1.50	15.2	15.4	15.5
1.60	14.9	15	15.2
1.75	14.5	14.5	14.8
2.00	13.6	13.6	13.9
2.25	12.8	12.6	13.2
2.50	12.3	11.8	12.6

[a] For the MP2/6-311g(d) method calculation, ONIOM(MP2/6-311g(d):B3LYP/6-311g(d)) were used;[17a] pyridine-d_5 is treated as high-layer and the 8T zeolite framework is treated as low-layer in the ONIOM calculation.

The smaller Mulliken charge on the H^+ ion will result in a larger shielding effect, and thus the position of the proton signal will shift to upfield, leading to a smaller ^{1}H chemical shift.[26] As shown in Tables 1 and 2, when pyridine adsorbs on the Brønsted site of zeolite with the acid strength increasing, the Mulliken charge on the acidic proton gradually decreases from 0.395 to 0.341 |e| and the ^{1}H chemical shift of the pyridine−H^+ ion successively decreases from 16.2 to 11.8 ppm predicted at B3LYP/DZVP2 level, which is in good agreement with the available ^{1}H NMR experimental data where a ^{1}H chemical shift in the range of 12−20 ppm is usually observed.[7−10] Generally, the stronger acid strength will result in a larger extent of proton transfer from zeolite to pyridine and a shorter N−H bond length. Because of the shorter H−N bond length, the positive charge will be more easily dispersed by the conjugate pyridine ring, and the pyridinium ion would have a smaller ^{1}H chemical shift.

In order to consider the effect of both computational methods and basis sets on the calculations, we also used B3LYP/6-311g(d) and MP2/6-311g(d) methods to predict the ^{1}H isotropic chemical shifts of adsorbed pyridine-d_5. The calculated results are also listed in Table 2. The ^{1}H chemical shifts calculated by the combinations of methods and basis sets follow the same variation trend that a smaller PA value (stronger acid strength) corresponds to a smaller ^{1}H chemical shift. A linear correlation (Figure 2) can be found between the ^{1}H chemical shift predicted by the three calculation approaches and the proton affinity, indicating that the ^{1}H chemical shift of adsorbed pyridine-d_5 can be used as a probe to measure the acid strength of solid acids. The good linear correlation does not deteriorate for the combinations of methods and basis sets (having a similar correlation coefficient value). It is noteworthy that the three calculation approaches predict the similar ^{1}H chemical shifts of solid acids with larger PA values, while the MP2/6-311g(d) method gives rise to a larger ^{1}H chemical shift of solid acids with smaller PA values compared with the B3LYP calculations. For the Si−H bond lengths at 2.25 and 2.50 Å (with the PA

TABLE 3: N−H Bond Length (r_{N-H}), Positive Charge Distribution of the H^+ and Pyridine−H^+ Fragments, BSSE-Corrected Adsorption Energies Predicted at the B3LYP/DZVP2 Level, and ^{1}H Chemical Shifts at MP2/6-311g(d) on an 8T Cluster Model for B−ZSM-5 and Al−ZSM-5 Zeolites[a]

model	r_{O-H}	PA	r_{N-H}	$Q_{(H^+)}$	$Q_{(pyridine-H^+)}$	E_{ads}	calcd ^{1}H	exptl ^{1}H
B−ZSM-5	0.965	320.2		0.3503				
Al−ZSM-5	0.971	301.6		0.38019				
B−pyridine	1.509		1.094	0.3986	0.8511	12.8	17.1	16.0
Al−pyridine	1.638		1.068	0.3910	0.9052	26.1	15.5	15.5

[a] Bond length in Å, adsorption energy in kcal/mol, charge in |e|, and chemical shift in ppm.

value being 263 and 254 kcal/mol, respectively), the calculated ^{1}H chemical shifts predicted at MP2/6-311g(d) level are 13.2 and 12.6 ppm, respectively, which are closer to the experimental value. The experimentally measured ^{1}H chemical shift is 13 ppm[27] for the pyridine-d_5 adsorption complex on the phosphotungstic acid $H_3PW_{12}O_{40}$ (with a PA value of 258.5 kcal/mol).[28] Therefore, the MP2/6-311g(d) provides a better prediction of the ^{1}H chemical shift of pyridine-d_5 adsorbed on much stronger acids (having smaller PA values).

It is well accepted that B−ZSM-5 zeolite has a weaker acid strength than Al−ZSM-5 as confirmed by the previous TPD−NH_3 and IR experiments.[19] Our calculated PA values also confirm this trend. As shown in Table 3, the larger PA (320.2 kcal/mol) and smaller adsorption energy of pyridine (12.8 kcal/mol) of B−ZSM-5 suggest that B−ZSM-5 has a much weaker acid strength compared with Al−ZSM-5, which is consistent with the experimental results.[19] The optimized structures of the two zeolites and the corresponding pyridine adsorption complexes are shown in Figure 1. The much longer zeolite−OH bond length (1.638 Å) and the much shorter N−H bond length (1.068 Å) in the pyridine adsorption complexes on Al−ZSM-5 compared with B−ZSM-5 (the two bond lengths are 1.509 and 1.094 Å, respectively) indicate a larger extent of proton transfer from the zeolites to adsorbed pyridine and thus a stronger acid strength of Al−ZSM-5. On the other hand, the different acid strengths of the two zeolites results in the different charge distributions in the adsorption complexes. The Mulliken charges on the pyridine−H^+ fragment are 0.8511 and 0.9052 |e| for B−ZSM-5 and Al−ZSM-5, respectively. However, the positive charge on the H^+ of B−ZSM-5 is about 0.008 |e| more than that of Al−ZSM-5 (see Table 3). The larger positive charge on the acidic proton of B−ZSM-5 results in a larger predicted ^{1}H chemical shift (17.1 ppm) compared with Al−ZSM-5 (15.5 ppm). The experimentally observed ^{1}H chemical shifts are 16.0 and 15.5 ppm for pyridine ions on B−ZSM-5 and Al−ZSM-5 zeolites, respectively.[10a,29] Therefore, it is further confirmed that

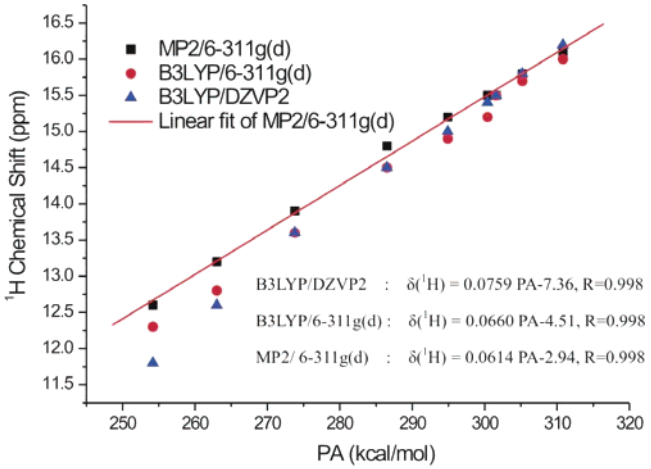

Figure 2. Correlation of calculated ^{1}H chemical shift of adsorbed pyridine-d_5 and proton affinity (PA) of solid acids.

TABLE 4: ^{1}H Chemical Shift of Pyridine-d_5 and ^{13}C Chemical Shift of Acetone-*2*-^{13}*C* Adsorbed on Different Solid Acids

	pyridine-d_5		acetone-*2*-^{13}*C*	
acid media	^{1}H chemical shifts (ppm)	ref	^{13}C chemical shifts (ppm)	ref
HSAPO-11	16.8	10c	217	10b
H-ZSM-5	19 and 15.5	10a	223	10b
$H_3PW_{12}O_{40}$	13	27	235 and 246	30
$AlCl_3$/MCM-41	12.5	10b	245 and 241	10b

for the pyridine adsorption on the solid acids, the stronger acid strength will result in a smaller ^{1}H chemical shift.

^{13}C NMR chemical shift of the carbonyl carbon of adsorbed acetone-*2*-^{13}*C* is a particularly sensitive probe to measure the strength of various solid acids (including zeolites), and the larger ^{13}C chemical shift indicates the stronger acid strength.[5] In Table 4, we list the ^{1}H chemical shift of pyridine-d_5 and ^{13}C chemical shift of acetone-*2*-^{13}*C* adsorbed on the different solid acids. For the strong solid acid, such as phosphotungstic acid $H_3PW_{12}O_{40}$ (PA = 258.5 kcal/mol),[28] a very small ^{1}H chemical shift (13 ppm)[27] and two large ^{13}C chemical shifts (235 and 246 ppm, with the latter corresponding to the threshold of superacidity) were observed for the adsorption complexes, indicative of an acid strength much stronger than that of H-ZSM-5.[30] For the weak solid acid, such as HSAPO-11 zeolite,[10c] a large ^{1}H chemical shift (16.8 ppm) and a small ^{13}C chemical shift (217 ppm) were observed, suggesting that the acid strength of HSAPO-11 is weaker than that of H-ZSM-5.[5b] For the H-ZSM-5 zeolite, two ^{1}H NMR signals at 15.5 and 19 ppm,[10a] due to pyridine-d_5 adsorbed on different Brønsted acid sites, can be observed, whereas the ^{13}C NMR of adsorbed acetone is unable to distinguish the acidic site distribution and an average chemical shift (223 ppm)[5] was observed.[31] The 15.5 ppm signal is attributed to pyridine-d_5 adsorbed on strong Brønsted acid sites, while the 19 ppm signal belongs to pyridine-d_5 adsorbed on weak Brønsted acid sites. Obviously, the ^{1}H chemical shift of pyridine-d_5 and the ^{13}C chemical shift of acetone-*2*-^{13}*C* adsorbed on the different solid acids can give rise to the same trend of acid strength order.

Since the ^{1}H chemical shift range of adsorbed pyridine-d_5 is relatively smaller (12−20 ppm) compared with the ^{13}C chemical shift range of adsorbed acetone-*2*-^{13}*C* (210−250 ppm),[5b] it may be expected that the ^{1}H NMR of adsorbed pyridine-d_5 is slightly less sensitive to solid acid strengths compared with the ^{13}C NMR of adsorbed acetone-*2*-^{13}*C*. However, as demonstrated in the present work, the ^{1}H chemical shift of adsorbed pyridine-d_5 can be used as a probe to measure the solid acid strength. The high detection sensitivity of ^{1}H NMR of adsorbed pyridine-d_5 and the easy assignment of ^{1}H NMR signals make it a fast and simple method for characterizing the Brønsted acid strength of solid acid catalysts which are widely used in the petrochemical industry.

Conclusion

The 8T zeolite model with different Si−H bond lengths is used to represent solid acids with different strength (from weak, strong to superacid), and the pyridine adsorption structure and the corresponding ^{1}H chemical shift are calculated. The DFT theoretical calculation demonstrates that there is a linear correlation between the ^{1}H chemical shift of adsorbed pyridine-d_5 and the PA value of solid acids, and thus the ^{1}H chemical shift can be used to characterize the solid acid strength. The smaller ^{1}H chemical shift of pyridinium ions on the solid acids corresponds to a stronger acid strength. The theoretical prediction is in good agreement with available experimental results.

Acknowledgment. This work was supported by the National Natural Science Foundation of China (20425311 and 20673139). We thank Shanghai Supercomputer Center (SSC) of China for its support and Professor M. Hunger for his valuable discussion.

References and Notes

(1) (a) Verhoef, M. J.; Creyghton, E. J.; Peters, J. A.; Bekkum, H. *Chem. Commun*. **1997**, 1989. (b) Wu, P.; Takayuki, K.; Tatsuaki, Y. *Microporous Mesoporous Mater.* **1998**, *22*, 343. (c) Corma, A.; Martinez-Triguero, J. *J. Catal.* **1997**, *165*, 102. (d) Souverijns, W.; Verrelst, W.; Vanbutsele, G.; Martens, J. A.; Jacobs, P. A. *J. Chem. Soc., Chem. Commun.* **1994**, 1671.

(2) (a) Barthos, R.; Lonyi, F.; Onyestyak, G.; Valyon, J. *J. Phys. Chem. B* **2000**, *104*, 7311. (b) Tessonnier, J. P.; Louis, B.; Walspurger, S.; Sommer, J.; Ledoux, M.; Pham-Huu, C. *J. Phys. Chem. B* **2006**, *110*, 10390.

(3) (a) Kao, H. C.; Yeh, M. *Microporous Mesoporous Mater.* **2002**, *53*, 1. (b) Peng, L.; Chupas, P. J.; Grey, C. P. *J. Am. Chem. Soc.* **2004**, *126*, 12254.

(4) Karra, M. D.; Sutovich, K. J.; Mueller, K. T. *J. Am. Chem. Soc.* **2002**, *124*, 902.

(5) (a) Haw, J. F.; Xu, T.; Nicholas, J. B.; Gorgune, P. W. *Nature* **1997**, *389*, 832. (b) Haw, J. F.; Nicholas, J. B.; Xu, T.; Beck, L. W.; Ferguson, D. B. *Acc. Chem. Res.* **1996**, *29*, 259.

(6) (a) Yang, J.; Zheng, A. M.; Zhang, M. J.; Luo, Q.; Yue, Y.; Ye, C. H.; Lu, X.; Deng, F. *J. Phys. Chem. B* **2005**, *109*, 13124. (b) Yang, J.; Zhang, M. J.; Deng, F.; Luo, Q.; Ye, C. H. *Chem. Commun.* **2003**, 884. (c) Luo, Q.; Deng, F.; Yuan, Z.; Yang, J.; Zhang, M. J.; Yue, Y.; Ye, C. *J. Phys. Chem. B* **2003**, *107*, 2435. (d) Ma, D.; Deng, F.; Fu, R.; Han, X.; Bao, X. *J. Phys. Chem. B* **2001**, *105*, 1770.

(7) Freade, D.; Hunger, M.; Pfeifer, H. *Chem. Phys. Lett*. **1982**, *91*, 307.

(8) Hunger, M. *Catal. Rev. Sci. Eng*. **1997**, *39*, 345.

(9) Hunger, M. *Solid State Nucl. Magn. Reson.* **1996**, *6*, 1.

(10) (a) Hunger, M.; Horvath, T.; Engelhardt, G.; Karge, H. G. In *Catalysis by Microporous Materials, Studies in Surface Science and Catalysis*; Beyer, H. K., Karge, H. G., Kiricsi, I., Nagy, J. B., Eds.; Elsevier: Amsterdam, 1995; Vol. 94, p 756. (b) Xu, M.; Arnold, A.; Buchholz, A.; Wang, W.; Hunger, M. *J. Phys. Chem. B* **2002**, *106*, 12140. (c) Chen, T.-H.; Wouters, B. H.; Grobet, P. J. *J. Phys. Chem. B* **1999**, *103*, 6179.

(11) Xu, J.; Zheng, A.; Yang, J.; Su, Y.; Wang, J.; Zeng, D.; Zhang, M.; Ye, C.; Deng, F. *J. Phys. Chem. B* **2006**, *110*, 10662.

(12) Kramer, G. J.; Vansanten, R. A.; Emeis, C. A.; Nowak, A. K. *Nature* **1993**, *363*, 529.

(13) (a) Zheng, X.; Blowers, P. *J. Mol. Catal. A* **2005**, *229*, 77. (b) Zheng, X.; Blowers, P. *J. Phys. Chem. A* **2005**, *109*, 10734.

(14) Chen, N. Y.; William R. G.; Frank, G. D. *Shape Selective Catalysis in Industrial Applications, Chemical Industries*; Marcel Dekker Inc.: New York, 1989; p 36.

(15) (a) Brand, H. V.; Curtiss, L. A.; Iton, L. E. *Phys. Chem.* **1993**, *97*, 7. (b) Pantu, P.; Pabchanda, S.; Limtrakul, J. *ChemPhysChem.* **2004**, *5*, 1901. (c) O'Malley, P. J.; Dwyer, J. *Zeolites* **1988**, *8*, 317.

(16) (a) Schroder, K. P.; Sauer, J.; Leslie, M.; Catlow, C. R. A. *Zeolites* **1992**, *12*, 20. (b) Alvarado-Swaisgood, A. E.; Barr, M. K.; Hay, P. J.; Redondo, A. *J. Phys. Chem.* **1991**, *95*, 10031. (c) Stave, M. S.; Nicholas, J. B. *J. Phys. Chem.* **1995**, *99*, 15046. (d) Xiong, J.; Ding, Y.; Zhu, H.; Yan, L.; Liu, X.; Lin, L. *J. Phys. Chem. B* **2003**, *107*, 1366.

(17) (a) Zheng, A. M.; Chen, L.; Yang, J.; Yue, Y.; Ye, C. H.; Lu, X.; Deng, F. *Chem. Commun.* **2005**, 2474. (b) Zheng, A. M.; Chen, L.; Yang, J.; Zhang, J. M.; Su, Y.; Yue, Y.; Ye, C.; Deng, F. *J. Phys. Chem. B* **2005**, *109*, 24273.

(18) van Koningsveld, H.; van Bekkum, H.; Jansen, J. C. *Acta Crystallogr. B* **1987**, *43*, 127.

(19) (a) Chu, C. T.; Cheng, C. D. *J. Phys. Chem. B* **1985**, *89*, 1569. (b) Yuan, S. P.; Wang, J. G.; Li, Y. W.; Peng, S. Y. *J. Mol. Catal. A: Chem.* **2002**, *178*, 267.

(20) Godbout, N.; Salahub, D. R.; Andzelm, J.; Wimmer, E. *Can. J. Chem.* **1992**, *70*, 560.

(21) Frisch, M. J.; Trucks, G. W.; Schlegel, H. B.; Scuseria, G. E.; Robb, M. A.; Cheeseman, J. R.; Montgomery, J. A., Jr.; Vreven, T.; Kudin, K. N.; Burant, J. C.; Millam, J. M.; Lyengar, S. S.; Tomasi, J.; Barone, V.; Mennucci, B.; Cossi, M.; Scalmani, G.; Rega, N.; Petersson, G. A.; Nakatsuji, H.; Hada, M.; Ehara, M.; Toyota, K.; Fukuda, R.; Hasegawa, J.; Ishida, M.; Nakajima, T.; Honda, Y.; Kitao, O.; Nakai, H.; Klene, M.; Li, X.; Knox, J. E.; Hratchian, H. P.; Cross, J. B.; Adamo, C.; Jaramillo, J.; Gomperts, R.; Stratmann, R. E.; Yazyev, O.; Austin, A. J.; Camml, R.; Pomelli, C.; Ochterski, J. W.; Ayala, P. Y.; Morokuma, K.; Voth, G. A.; Salvador, P.; Dannenberg, J. J.; Zakrzewski, V. G.; Dapprich, S.; Daniels, A. D.; Strain, M. C.; Farkas, O.; Malick, D. K.: Rabuck, A. D.; Raghavachari, K.; Foresman, J. B.; Ortiz, J. V.; Cui, Q.; Baboul, A. G.; Clifford, S.; Cioslowski, J.; Stefanov, B. B.; Liu, G.; Liashenko, A.; Piskorz, P.; Komaromi, I.; Martin, R. L.; Fox, D. J.; Keith, T.; Al-Laham, M. A.; Peng, C. Y.; Nanayakkara, A.; Challacombe, M.; Gill, P. M. W.; Johnson, B.; Chen, W.; Wong, M. W.; Gonzalez, C.; Pople, J. A. *Gaussian03*, revision B.05; Gaussian, Inc.: Pittsburgh, PA, 2003.

(22) Nicholas, J. B. *Top. Catal*. **1999**, *9*, 181.

(23) Boronat, M.; Viruela, P. M.; Corma, A. *J. Am. Chem. Soc.* **2004**, *126*, 3300.

(24) The Si-H bond length is set to 1.470, 1.4837 and 1.490 Å in the refs 17b, 5a and 23, respectively.

(25) Brand, H. V.; Curtiss, L. A.; Iton, L. E. *J. Phys. Chem.* **1993**, *97*, 12773.

(26) Mehring, M. *High Resolution NMR in Solids*, 2nd ed.; Springer-Verlag: New York, 1983.

(27) Oshihide, B.; Mamoru, N.; Yoshio, O.; Yoichi, O. *J. Phys. Chem.* **1993**, *97*, 12888.

(28) Janik, M. J.; Davis, R. J.; Neurock, M. *Catal. Today* **2005**, *105*, 134.

(29) Reddy Marthala, V. R.; Wang, W.; Jiao, J.; Jiang, Y.; Huang, J.; Hunger, M. *Microporous Mesoporous Mater.* **2007**, *99*, 91.

(30) Yang, J.; Janik, M. J.; Ma, D.; Zheng, A.; Zhang, M.; Neurock, M.; Davis, R. J.; Ye, C.; Deng, F. *J. Am. Chem. Soc.* **2005**, *127*, 18274.

(31) Biaglow, A. I.; Gorte, R. J.; White, D. *J. Catal.* **1994**, *148*, 779.